Published in final edited form as:
Biochim Biophys Acta. 2016 February ; 1863(2): 205–218. doi:10.1016/j.bbamcr.2015.10.023.

Sequence-function correlations and dynamics of ERG isoforms. ERG8 is the black sheep of the family

Bastian Hoesel[#], **Naila Malkani**[#], **Bernhard Hochreiter**, **José Basílio**, **Kalsoom Sughra**, **Muhammad Ilyas**, and **Johannes A. Schmid**[*]
Dept. of Vascular Biology and Thrombosis Research, Center for Physiology and Pharmacology, Medical University of Vienna, Austria

[#] These authors contributed equally to this work.

Abstract

The transcription factor ERG is known to have divergent roles. On one hand, it acts as differentiation factor of endothelial cells. On the other hand, it has pathological roles in various cancers. Genomic analyses of the *ERG* gene show that it gives rise to several isoforms. However, functional differences between these isoforms, representing potential reasons for distinct effects in diverse cell types have not been addressed in detail so far. We set out to investigate the major protein isoforms and found that ERG8 contains a unique C-terminus. This isoform, when expressed as GFP-fusion protein, localized mainly to the cytosol, whereas the other major isoforms (ERG1-4) were predominantly nuclear. Using site directed mutagenesis and laser scanning microscopy of live cells, we could identify nuclear localization (NLS) and nuclear export sequences (NES). These analyses indicated that ERG8 lacks a classical NLS and the DNA-binding domain, but holds an additional NES within its distinctive C-terminus. All the tested isoforms were shuttling between nucleus and cytosol and showed a high degree of mobility. ERG's 1 to 4 were transcriptionally active on ERG-promoter elements whereas ERG8 was inactive, which is in line with the absence of a DNA-binding domain. Fluorescence resonance energy transfer (FRET) microscopy revealed that ERG8 can bind to the transcriptionally active ERG's. Knockdown of ERG8 in endothelial cells resulted in upregulation of endogenous ERG-transcriptional activity implying ERG8 as an inhibitor of the active ERG isoforms. Quantitative PCR revealed a different ratio of active ERG's to ERG8 in cancer- versus non-transformed cells.

Keywords

ERG; ETS transcription factor family; DNA binding protein; Nuclear localization sequence; Nuclear export sequence; Microscopy; Fluorescence recovery after photobleaching (FRAP); Fluorescence resonance energy transfer (FRET)

[*]Corresponding author at: Dept. of Vascular Biology and Thrombosis Research, Center for Physiology and Pharmacology, Med. Univ. Vienna, Austria, Schwarzspanierstr, 17, 1090 Vienna, Austria. Tel.: +43 1 40160 31155; fax: +43 1 40160 931101. johannes.schmid@meduniwien.ac.at (J.A. Schmid).

Transparency document
The Transparency document associated with this article can be found, in online version.

Appendix A. Supplementary data
Supplementary data to this article can be found online at http://dx.doi.org/10.1016/j.bbamcr.2015.10.023.

Europe PMC Funders Author Manuscripts

1. Introduction

ERG (ETS-related gene) is a member of the ETS-family of transcription factors, which are characterized by a helix–turn–helix DNA binding domain, and recognizes a highly conserved DNA binding sequence of purine rich nucleotides GGAA/T [1]. When first reported in 1987, ERG was shown to have two variants [2]. This number was significantly increased later, when Owczarek et al., analyzed the genomic structure of ERG on chromosome 21 in more detail using improved detection methods, which led to the notion that ERG has at least 17 exons and 16 introns resulting in about 9 isoforms, which are the consequence of alternative splicing [3]. Very recently an even more elaborate analysis of the ERG variants has been published [4], which considers three alternative promoters, two splice sites, three separate polyadenylation sites and a variety of different translation start sites resulting in about 30 possible ERG variants, of which only a subset is usually expressed on the protein level. This latter analysis is the most elaborate and detailed description of ERG-isoforms. We set out to analyze five of the major ERG isoforms as specified in Fig. 2A including ERG8, which differs significantly from the other isoforms since it is lacking the DNA binding domain and has a very distinct and unique C-terminus.

Despite the fact that the *ERG* gene is expressed in distinct isoforms with potentially different functions, ERG is considered in most reports as a single entity. *ERG* is physiologically highly expressed in the endothelium where it is involved in vasculogenesis [5], angiogenesis [6] and overall cell maintenance [7]. The expression of several endothelial cell specific genes is under the control of ERG such as VE-cadherin [8], endoglin [9] and Van-Willebrand factor [10]. Moreover it has also been proposed that ERG regulates endothelial cell barrier functions and that it suppresses inflammation by regulating the expression of Claudin-5 [11], ICAM-1 [12] and IL-8 [13]. This anti-inflammatory effect was reported to correlate with a reduced serine-536 phosphorylation of p65 NF-κB [12]. Besides the physiological expression of ERG in endothelial and hematopoietic cells, it is also pathologically expressed in about 50% of prostate cancer patients due to a fusion of the *ERG* gene with a prostate-specific promoter [14]. Furthermore, disease related expression of ERG or ERG-fusion genes is observed in certain types of leukemia [15] and in Ewing sarcoma [16].

In contrast to the inflammation dampening effect of ERG in endothelial cells, it was reported to act as a pro-inflammatory mediator in prostate cancer cells, where it enhanced phosphorylation of p65 serine-536 [17]. Since ERG occurs in a variety of isoforms and different fusion proteins, an elucidation of its dissimilar biological functions in diverse cell types requires a more detailed analysis of the differences in protein sequence and domain structure. Furthermore, it is important to note that ERG-variants have the ability to form homo- or heterodimers generating an even higher functional diversity [18,19]. Since a complete understanding of the diverse functions of the various ERG isoforms is still lacking, we set out to characterize the major protein isoforms in more detail based on an elaborate analysis of differences in sequence and functional domains and correlating biological functions.

2. Materials and methods

2.1. Cell culture and transfections

Primary human umbilical vein endothelial cells (HUVEC), lymphatic endothelial cells (LEC) and SV40 immortalized HUVECs (TERT-HUVECS) were cultivated in M199 medium as described [20]. All other cell lines (VCaP, HEK293, HeLa, KG-1 and EA.hy926) were maintained in DMEM medium supplied with 10% FBS. Transient cell transfections were performed with Turbofect™ (Thermofisher, Germany) as recommended by the manufacturer; HUVECs were transfected with polyethylenimine as described in [21].

2.2. Gene expression and suppression constructs

cDNA from HUVEC and PCR were used to generate constructs for ERG1, ERG3, ERG4 and ERG8 isoforms. The primers used to generate these isoforms contained HindIII and SalI sites for cloning into the pEGFP-C1 vector (Clontech, USA) resulting in EGFP–ERG1, EGFP–ERG3, EGFP–ERG4 and EGFP–ERG8. The sequences of the primer sets are described in Suppl. Table 1. PCR products were gel purified, digested with HindIII and SalI and ligated into pEGFP-C1 digested with the same enzymes. ERG1b was amplified by primers containing BglII and EcoRV sites (Suppl. Table 1), inserted into the pGEM-T Easy vector (Promega Inc. Madison, WI, USA.), cut out from the vector with BglII and EcoRV and inserted into pARR2PB-Bluescript, a vector containing the prostate-specific, androgen dependent promoter ARR2PB, obtained from R. Matusik [22]. EGFP–ERG1b was then obtained by cutting out ERG1b from ARR2PB–ERG1b with Bgl II and Dra III and ligating the insert into pEGFP–p65 [23], cut with the same enzymes, thereby replacing p65 with Erg1b. All constructs were confirmed by sequencing before use. The nuclear localization sequence mutant (EGFP–ERG1b–ΔRKSK) was generated by a deletion PCR reaction eliminating amino acids 337 to 340. For a mutation of the putative common N-terminal nuclear export signal(s) the leucines at position 207 and 210 in ERG1b and ERG8 were mutated to arginine using appropriate mutation primer sets. The second putative nuclear export sequence, which is unique for ERG8, was mutated using appropriate mutation primer sets (Suppl. Table 1). The PNT truncated ERG8 protein was generated by a deletion of the major part (amino acid 141 (W) to amino acid AA 183 (F)) of the PNT domain using appropriate primers sets. Two additional ERG mutants were generated, designated as W235R and RRAA. W235R, harbors a single amino acid mutation close to the DNA binding domain (replacing tryptophan-235 with arginine). For the RRAA mutant two positively charged arginine residues of the core DNA binding sequence of ERG (KLSRALR) as defined by the crystal structure of ERG bound to DNA [24] were mutated to alanines. These two mutants were generated with the QuikChange mutagenesis kit (Stratagene, Santa Clara, CA) using the mutation primers as specified in Suppl. Table 1. A gene suppression construct targeting specifically ERG8 was designed using the online siDesign Center of Dharmacon (GE Life Sciences Inc) at http://dharmacon.gelifesciences.com/design-center/ with the unique C-terminus of ERG8 as input. The candidate with the highest score was selected and ordered as chemically synthesized siRNA from Microsynth AG, Balgach, Switzerland with dTdT overhangs. A scrambled proven non-functional siRNA was used as control. The sequences were as follows:

siERG8: sense: 5′-CUG UUG AUU UGG AGA CUA ATT, antisense: 5′-UUA GUC UCC AAA UCA ACA G,

control-siRNA: sense: 5′-CGA GGA CUC UGA AUA GUG U, antisense: 5′-ACA CUA UUC AGA GUC CUC G.

2.3. Reporter gene assays

A luciferase reporter construct suited for determining the transcriptional activity of ERG variants was generated by inserting three copies of the ERG consensus binding sequence into the vector pGL4.14 (from Promega, USA). To that end, the following oligonucleotides were used:

Sense: 5′-
CTAGCACAGGAAGATATCTACGGACAGGAAGCGATAAGCCTACAGGAAA-3′

Antisense: 3′-
GTGTCCTTCTATAGATGCCTGTCCTTCGCTATTCGGATGTCCTTTCTAG-5′

(sequences are shown as annealed double-stranded oligonucleotide to emphasize the sticky ends fitting to the restriction sites of the entry vector; underlined: ERG-core binding region). These oligonucleotides were annealed by mixing them at a concentration of 50 μg/μl followed by incubation at 95 °C for 10 min in an Eppendorf thermomixer, and slow cooling of the solution. The annealed oligonucleotides were ligated into a pGL4.14 vector cut with Bgl II and Nhe I. An improved luciferase reporter construct for ERG activity (3× ERG-Nanoluc) was generated with the same procedure by inserting the annealed double-stranded oligonucleotide into a pNanoluc 1.1 vector (Promega Inc.). Luciferase reporter constructs were transfected in combination with a constitutively expressing β-Galactosidase construct (driven by a ubiquitin-promoter: pUB6/V5-His/lacZ from Life Technologies, Austria) or with a constitutively expressing GFP-vector (pEGFP-C1, Clontech Inc. containing a CMV-promoter) for normalization purposes together with ERG isoform specific expression or gene suppression constructs. Cell extracts were prepared and normalized luciferase activities were measured as described in [23]. For measurements of ERG-dependent Nanoluc activity, the substrate and protocol of the manufacturer (Promega Inc.) was used.

2.4. Microscopy techniques

Confocal laser scanning microscopy was performed on Zeiss LSM510 META and on Nikon A1 R + equipment. FLIP (fluorescence loss in photobleaching) and FRAP (fluorescence recovery after photobleaching) were used to study the dynamics of ERG isoforms. Cells were grown on 15 mm round glass cover slips (0.17 mm thick), transfected with EGFP-tagged versions of proteins one day after seeding and analyzed on the next day. Cover slips were mounted on a self-made aluminum incubation chamber containing 80 μl medium and analyzed as described in [25]. For detection and visualization of protein interactions, we performed FRET (Fluorescence resonance energy transfer) microscopy according to the 3-filter methodology as described in [26]. FRET microscopy was done with living cells expressing EGFP- and mDsRed-tagged fusion proteins using a Zeiss LSM510 META system and appropriate dichroic mirrors and filters sets. Monomeric DsRed was detected

with the spectral channel ChS1, GFP captured with channel 2 and the raw FRET signal acquired on channel 3 to obtain maximum sensitivity for FRET. For FLIP analysis of nucleo-cytoplasmic shuttling, the slide was placed on the stage of a Zeiss LSM510 META microscope and cells were observed with a 40× oil immersion objective (numerical aperture 1.3). Moderately fluorescent cells were selected for analysis and a circular region of interest was defined in the cytoplasm. The cell was imaged at low laser power (Ar-488 nm line, 6%) followed by 50 bleaching cycles with high laser power (Ar-488 nm line, 100%) and subsequent image acquisition of the whole cell as before. Approximately 5 cells were monitored and cytosolic as well as nuclear fluorescence intensities were quantified using ImageJ software. This analysis allows a quantitative evaluation of the shuttling between nucleus and cytosol [27]. In order to determine the mobility of ERG isoforms within the nucleus, FRAP experiments were performed as described [28] using a circular region of interest in the nucleus for bleaching. A Zeiss LSM510 system was applied with a 40× oil immersion objective and numerical aperture of 1.3. First a pre-bleaching image of a whole cell was acquired at low laser power (6%) followed by 50–100 bleach cycles of the defined region at high laser power (Ar-488 nm, 100%), and a subsequent time series of the bleached region of interest at low laser power (Ar-488 nm, 6%). By scanning only the bleached region, a high time resolution could be obtained. After this series, a post-bleaching image of the whole cell was acquired to determine the overall loss of fluorescence. In the bleached area the recovery of the fluorescence was calculated using ImageJ. The loss of fluorescence from pre-bleaching image to post-bleaching image was used to calculate a correction factor so that a correct recovery phase could be determined.

2.5. DNA binding assay (ABCD)

ABCD (Avidin Biotin Complex with DNA) assays were principally performed as described [29,30]. In brief, HEK293 cells were transfected with various ERG isoforms in 10 cm^2 cell culture dishes. 24 h after transfection cells were washed with PBS, centrifuged and resuspended in 1 ml of NTEN lysis buffer (10 mM Tris pH 8,0; 100 mM NaCl; 1 mM EDTA pH 8,0; 10% glycerol; 0,5% Nonidet; 1 mM DTT), sonicated and centrifuged. The pellet was discarded and 200 µl of cell lysates were incubated with 2 µl of biotinylated oligonucleotides (50 µg/µl) containing four ERG-consensus binding sites. Lysate/ oligonucleotide mixtures were then incubated with 40 µl streptavidin-conjugated agarose beads (Novagen, USA), followed by 5× washing with 50 mM KCl at 4 °C, removal of bound proteins with SDS-buffer by incubation for 5 min at 95 °C and separation by SDS-PAGE using 10% polyacrylamide gels. Sequences of oligos used for ABCD assay were:

Sense: Biotin-5′-ACCGGAAGTGACCGGAAGTGACCGGAAGTGACCGGAAGT-3′ (binding sites are underlined).

Antisense: biotin — 5′ ACTTCCGGTCACTTCCGGTCACTTCCGGTCACTTCCGGT 3′.

The same oligonucleotides without a biotin label were used as a competitor control in 10-fold molar excess. Moreover, specificity of the ABCD assay was assessed by using an ERG core-binding mutant (RRAA, Fig. 6). Immuno-blotting was performed on PVDF-membranes and ERG-isoforms were detected using antibodies (SantaCruz Biotechnology, USA, sc-353 X (ERG), or sc-8334 (GFP)) according to the manufacturer's protocol. Of

note, ERG8 was not detectable with an ERG specific antibody, most likely because it is lacking the C-Terminus, which contains the DNA-binding domain. Incubation of the lysates with streptavidin beads in absence of any oligonucleotide served as negative control to test for unspecific binding to the beads. Cell lysates themselves were applied to the gel as positive control to verify the expression of the transcription factor.

2.6. Quantitative PCR analysis of ERG isoforms

We used isoform specific qPCR primers for the detection of each isoform in cell lines. The reaction was performed in a final volume of 20 µl using a SYBR green qPCR master mix (Thermofisher, Germany). Normalization was done using specific primers for GAPDH. The primer sequences used are provided in Suppl. Table 2. The analysis was done by using LinReg PCR software [31], which calculates the PCR efficiency of each amplicon after determining the baseline fluorescence. Relative quantification as compared to a control sample was calculated according to [32]. Specific primers for ERG3 were not possible to design due to the homologies with other isoforms. To address that, we used primers that amplify all ERG isoforms (pan-ERG primers), calculated Cq values for total ERG and subtracted the values of ERG1, 1b, −4, −7 and −8 to get the value for ERG3 and all other potential isoforms. For Fig. 10, we calculated the total amount of active ERGs by subtracting total ERG from ERG8 expression relative to GAPDH and used these values to calculate the ratio of active ERG/ERG8.

2.7. Statistics

Error bars represent S.E.M. if not stated differently. Numbers of replicates (n-values) are specified in the figure legends. Unpaired t-tests with two-tailed P-values were used for comparison of two groups. One-way ANOVA with Dunnett's multiple comparison test was used for Fig. 10. Statistical analysis was done with *GraphPad Prism 5.0* or *6.0* software.

3. Results

3.1. Localization of ERG isoforms

Since antibodies discriminating between the ERG variants are not available, we generated GFP-tagged fusion proteins of the isoforms so as to localize them in living cells. Expression constructs were transfected into HEK293 cells and 24 h after transfection, moderately expressing cells were analyzed by confocal laser scanning microscopy. ERG isoforms 1, 1b, 3 and 4 were predominantly found in the nucleus with some weak fluorescence in the cytosol, while ERG isoform 8 was mainly localized to the cytoplasm (Fig. 1A). A quantification of the distribution between nucleus and cytoplasm for a higher number of cells confirmed the notion that ERG8 differs significantly from the other isoforms by localizing primarily in the cytoplasm (Fig. 1B).

3.2. Nuclear localization and nuclear export sequences of ERG isoforms

The result of the microscopy of cells transfected with GFP-tagged expression constructs of the various ERG-isoforms prompted us to search in more detail for potential nuclear localization sequences (NLS) and nuclear export signals (NES) in the amino acid chains of the ERG-variants. We identified a RKSK-sequence in the ETS domain as a potential nuclear

localization sequence in ERG isoforms 1, 1b, 3 and 4, which is absent in ERG8 (Fig. 2A, marked in red). This putative NLS is in a region that is very homologous for the different members of the ETS family. The crystal structure of the ETS-1 protein, shows a conserved, ERG-homologous sequence (RKNK) close to the helix that binds to the major groove of the DNA (structure 2NNY, [33]). The very recent elucidation of the DNA-bound structure of ERG itself [24] is in line with that and presents the putative NLS close to the DNA-binding domain (structure 4IRI, Fig. 2B). ERG8 differs significantly from all the other isoforms by lacking the conserved ETS domain, which contains the nuclear localization signal and the DNA-binding domain. Instead it holds a short, particularly distinct C-terminus. Based on the published information of functional domains, the sequence analysis furthermore indicated that isoforms 1 to 4 possess two transactivation domains whereas ERG8 contains only one of these.

In addition to nuclear localization signals, we also searched for potential nuclear export signals in the amino acid sequences of the major ERG isoforms as many transcription factors shuttle between nucleus and cytosol. Nuclear export of proteins relies primarily on the NES-receptor Crm1p and usually depends on a stretch of hydrophobic residues, such as leucines or isoleucines separated by 1–4 amino acid spacer domains [25,34,35]. Such a potential nuclear export signal was observed at the amino acid position 207 of all investigated ERGs. Interestingly, ERG8 contains an additional potential NES, which is characterized by a stretch of leucines within its distinct C-terminus (Fig. 2A).

To first test the functional role of the putative NLS of ERG isoforms 1–4, we deleted the potential NLS in a GFP-tagged expression construct of a representative isoform (ERG1b) and transfected the mutated plasmid into HEK293 cells. As expected, the nuclear localization of this mutant was considerably reduced as compared to the wild-type protein, which was paralleled by an increase of cytoplasmic fluorescence (Fig. 3A). Quantification of that effect for a higher number of cells revealed a significant decrease of the ratio of nuclear to cytoplasmic fluorescence in RKSK mutant cells as compared to cells transfected with wild-type EGFP–ERG1b (Fig. 3B).

We next tested the functionality of the predicted nuclear export sequences. To that end, we first mutated the leucines at position 207 and 210 of ERG8 to destroy the postulated common first NES. The second NES, which is specific for ERG8, was generated by mutating the leucines at position 297 and 302. Mutation of the first or second putative NES both resulted in a reduction of ERG8 cytosolic localization and an increase in nuclear ERG8 implying that both NES sequences are functional in this isoform (Fig. 4A, B). Interestingly, we did observe that a mutation of the second NES leads to a stronger reduction of the cytosolic to nuclear localization of ERG8 as compared to a mutation of the first NES (Fig. 4B). We thus tested whether the mutation of both NES sequences has a synergistic effect on the ERG8 protein localization. The cytosolic to nuclear ratio was, however, not significantly different in the double NES mutant, as compared to the second NES mutant alone (Fig. 4B), suggesting that the second NES, which is specific for ERG8, has a stronger effect than the first NES, which is present in all the tested isoforms. Furthermore we also tested whether a deletion of the PNT domain of ERG8 has an effect on its cytosolic localization. However,

we could not observe any significant influence of this mutation on the subcellular distribution of ERG8 (not shown).

In order to test, whether the first potential NES, which is present in all the ERG isoforms, is functional as well, we mutated this region in EGFP–ERG1b by replacing the first two leucine residues. Since ERG1–4 are already predominantly nuclear at steady state, a further increase in nuclear localization by mutating this NES is hardly visible (Suppl. Fig. 1). To solve that issue, we applied a technique designated as fluorescence loss in photobleaching (FLIP) microscopy, where one compartment (the cytosol) is repetitively bleached by a strong laser, followed by imaging of the whole cell at low laser excitation. A decrease of the fluorescence intensity in a non-bleached compartment (such as the nucleus) indicates dynamic shuttling of the fluorescent protein between the two compartments. Such an approach can be exploited to prove the functionality of a NES, as the nuclear fluorescence of a shuttling protein decreases upon bleaching of the cytosol and this decrease should be significantly reduced by mutation of a functional NES. Applying this technique to ERG1b and ERG1b with a mutated putative NES could clearly show that the postulated NES is functional, causing constitutive nucleo-cytoplasmic shuttling in this ERG isoform (Fig. 4C, D and Suppl. Fig. 2). FLIP experiments with the other major ERG isoforms demonstrated that all of them shuttle between nucleus and cytosol (Fig. 4E). This was also true for the mutants of the first and the second NES of ERG8, as well as the double NES mutant supporting the notion that both NES are functional in ERG8 (Suppl. Fig. 3). This data also indicates that there are other mechanisms controlling the ERG8 cytosolic ratio. The fact that ERG8, which lacks a classical NLS is also present to a minor extent in the nucleus and furthermore exhibits shuttling between nucleus and cytosol implies the presence of a non-classical, rather weak NLS in this isoform.

3.3. Mobility of ERG isoforms in the nuclei of living cells

For further investigation of the dynamics of ERG isoforms another microscopy technique termed FRAP (Fluorescence Recovery after Photobleaching) was applied. This technique is suited to monitor the mobility of a fluorescent protein within a given compartment in living cells. We performed this microscopy technique on HEK293 cells expressing EGFP-tagged ERG1, 1b, 3, 4 or 8 as described in the Methods section. While ERG8 was predominantly expressed in the cytosol, a smaller fraction was also visible in the nucleus. For reasons of comparison with the other isoforms, we therefore determined the mobility of ERG8 in the nucleus as well. An area of interest in the nucleus was defined, scanned at low laser intensity, followed by bleaching at full laser power and subsequent time-lapse imaging of the bleached area at low laser excitation. The fluorescence recovery in the region as a result of diffusion of molecules from outside into the bleaching area was monitored and quantified over time (Fig. 5). The resulting fluorescence intensities over time could be fitted with an exponential increase algorithm resulting in the calculation of a plateau value and a half-life of recovery. The first parameter usually defines the percentage of generally mobile molecules within that time window, and the second parameter is a measure of the diffusion rate [28]. This analysis revealed clear differences between the ERG variants with ERG8 being the most mobile of all tested isoforms. The overall mobility of ERG isoforms 1, 1b and 3 was almost the same as indicated by nearly identical fitted plateau values. The half-

life of recovery appeared to be lower for ERG8 as compared to ERG 1, 1b and 3, meaning ERG8 is more mobile as compared to other isoforms (Fig. 5).

3.4. DNA-binding and transcriptional activities of ERG isoforms

Based on the sequence comparison shown in Fig. 2A, where ERG8 appeared to lack a functional DNA binding region within the ETS domain, we aimed at testing the DNA-binding capabilities of the ERG isoforms. To that end, we applied ABCD (Avidin-Biotin Complex with DNA) assays as alternatives to radioactive EMSA's (electrophoretic mobility shift assays). The isoform constructs were transfected into HEK293 cells and whole cell lysates were tested for their binding activities to double-stranded biotinylated oligonucleotides containing the consensus ERG-binding sequence. This assay revealed that ERG isoforms 1, 1b, 3 and 4 bind specifically to the ERG binding sites as expected. However, in the case of ERG8, the pull-down of the biotinylated oligonucleotide with streptavidin-beads did not show any significant binding of ERG8-protein (Fig. 6A, Fig. 9A, B). Furthermore, we included an ERG-variant with a mutation in the DNA binding domain (replacing two arginines by alanines, termed RRAA-mutant) as a control, which also did not show any significant DNA binding. Combining this result with the fact that ERG8 lacks the DNA-binding domain known from crystal structure analysis [24] led us to the conclusion that ERG8 is not specifically binding to DNA and is therefore not acting as transcription factor. For a further elucidation of the transcriptional activities of the major ERG isoforms, we performed luciferase assays using a reporter construct containing three consensus-binding sites for ERG. Transfection of cells with this construct in combination with ERG1, 1b, 3, 4 or 8 showed that ERG isoforms 1–4 acted as functional transcription factors, while ERG8 did not show any significant transcriptional activity (Fig. 6B). Two non-functional variants of ERG (RRAA, W235) with mutations in the DNA binding domain were again used as control. We confirmed expression of the different isoforms in the samples used for luciferase assays on a Western blot (Fig. 6C). Since ERG8 protein is not detectable with a normal ERG antibody, we also used a normal GFP antibody to confirm ERG8 protein expression (Fig. 6D).

3.5. ERG8 interacts with other ERG isoforms

It has been postulated that ERG-protein isoforms can form homo- or heterodimers with other isoforms [36] or even other transcription factors such as Jun. [19]. To test for potential protein interactions between the transcriptionally active ERG isoforms and ERG8, we transfected GFP-tagged ERG isoforms 1, 1b, 3 and 4 along with mDsRed-ERG8 in HEK293 cells and performed FRET (fluorescence resonance energy transfer) microscopy in living cells. This analysis revealed that ERG8 is able to interact with all the active isoforms and that this interaction occurred primarily in the cytosol (Fig. 7). Despite the fact that we observed a significant FRET signal and thus a physical interaction between ERG8 and the other ERG-isoforms, we did not see a substantial shift of the localization of the active isoforms from the nucleus towards the cytosol. Just the fraction of the ERGs that localized to the cytosol appeared to interact with ERG8. Co-expressing two differentially tagged active isoforms (ERG1 and ERG3) showed an interaction in the nucleus as expected.

3.6. Effect of ERG8 expression on the transcriptional activity of the other ERG isoforms

Since ERG8 could interact with the other ERG isoforms and was transcriptionally inactive, we speculated that ERG8 could function as an inhibitor of the other ERG isoforms. We thus first transfected HEK293 cells with ERG1-4 alone or together with ERG8 and determined luciferase activity of an ERG dependent promoter. Using this approach, we could detect a significant reduction of the normalized ERG-dependent luciferase activity for ERG1, 1b, 3 and 4 in the presence of ERG8 (Suppl. Fig. 4). However, when we determined ERG protein levels by Western blot in these samples we could detect a reduction of ERG 1-4 protein levels in the ERG8 co-transfected samples (Suppl. Fig. 4). The reduced expression of active ERGs upon transfection with ERG8 might be either an indirect transfection effect or an influence of ERG8 on the expression of the active ERG isoforms. In order to prevent an overexpression effect, we decided to test a potential functional role of ERG8 by a specific knockdown in ERG-positive cells. To that end, we designed a siRNA sequence that targets the unique C-terminus of ERG8. The specificity of the ERG8 gene suppression was confirmed by co-transfecting ERG8-siRNA or a scrambled control-siRNA with GFP-tagged expression constructs of ERG-isoforms (Suppl. Fig. 5). Transfecting endothelial cells (HUVECs) with control- or ERG8-siRNA in combination with an ERG-dependent improved luciferase construct (Nanoluc) revealed a significant increase in endogenous ERG-activity upon knockdown of ERG8 when normalized to co-transfected GFP (Fig. 8A). Interestingly, the expression of endogenous active ERG (primarily ERG3, as assessed by qPCR, Suppl. Fig. 6) increased significantly, when ERG8 expression was suppressed (Fig. 8B). Nevertheless, normalizing ERG-dependent luciferase activity to the ERG-protein band intensity still revealed a significant upregulation of ERG-dependent transcriptional activity after knockdown of ERG8 (Fig. 8C) implying an inhibitory role of ERG8 in these cells.

3.7. ERG8 reduces DNA binding of ERG1b in vitro

As we found a higher ERG activity after gene suppression of ERG8, we wanted to test, whether ERG8 interferes with DNA-binding of a transcriptionally active ERG isoform. To that end, we performed *in vitro* DNA-binding assays with increasing amounts of ERG8 and constant amounts of ERG1b. HEK293 cells were transfected either with ERG1b or with ERG8 and cell extracts were mixed at different ratios before adding biotinylated oligonucleotides with ERG-binding sequences and pull-down with streptavidin-beads, followed by Western blot analysis of precipitated ERG-protein. Using this approach, we detected a decrease of DNA-bound ERG1b with increasing levels of ERG8 (Fig. 9A, C). However, this effect was rather mild implying that additional mechanisms account for the biological effect of ERG8.

3.8. The expression of active ERG isoforms versus ERG8 differs between cancer and endothelial cells

Since there are no antibodies available that differentiate between the distinct ERG isoforms on the protein level, we aimed to distinguish between the isoforms on the mRNA level. To that end, we designed primers that are specific for the different major isoforms based on the published mRNA-sequences and analyzed their expression in various endothelial and cancer cell lines. Quantitative PCR analyses indicated that the isoforms 1–4 and 8 are differentially

expressed in these cells while isoforms 5 and 7 could not be detected in any of the cell lines tested (Suppl. Fig. 6). Interestingly, our analyses revealed that there was a difference in the ratio of active ERG's to ERG8 in the cells tested. We quantified the ratio of active ERG's to ERG8 in primary endothelial cells from veins (HUVECs), lymphatic vessels (LEC), SV40 immortalized HUVECS (TERT-HUVECS), cancer-like endothelial hybridoma cells (EA.hy 926, ATCC CRL-2922), the ERG-positive prostate cancer cell line VCaP, in HeLa cells and the human acute myeloid leukemia cell line KG-1. Interestingly, the active ERG to ERG8 ratio was significantly higher in endothelial cells as compared to all the three cancer cell lines (Fig. 10). Furthermore, we could observe a reduction of the ERG to ERG8 status in the cancerous endothelial hybridoma cell line EA.hy 926, as compared to non-transformed endothelial cells. Statistical analysis revealed no significant difference between the three non-transformed endothelial cell types and no difference within the cancer cell lines, but a significant difference between the cancer cell lines and the benign cell types.

4. Discussion

ERG, a member of the ETS family of proteins, regulates the expression of many endothelial-specific genes like VE-Cadherin, ICAM-2, VWF or VEGFR1 [37] and knockdown studies indicated that it is involved in endothelial cell proliferation, migration and angiogenesis [8] [38]. Apart from its physiological role in endothelial cells, ERG is also aberrantly expressed either alone or as a fusion protein in a variety of cancers. The genomic structure of the ERG gene indicates alternative splicing, as well as several start codons and polyadenylation sites resulting in a plethora of possible ERG isoforms, which might have different functions and account for differences of ERG-effects in distinct cell types. We set out to investigate the major ERG isoforms in more detail and to identify potential functional differences based on sequence variations. Since no antibodies are available that would differentiate between the isoforms, we generated GFP-tagged expression constructs of the major ERG isoforms ERG1, −1b, −3, −4 and −8 and monitored the localization of the chimeric proteins after transfection. Confocal laser scanning microscopy of live cells revealed a predominant nuclear localization for isoforms 1–4, as expected from other studies [13]. Some moderate occurrence in the cytoplasm could also be observed for these isoforms, which has also been reported previously [39]. In contrast to that, ERG8 was primarily localizing to the cytosol. This finding was corroborated by more detailed sequence analyses and alignment of ERG-isoforms, suggesting the presence of a classical NLS in the ETS domain of ERG1–4, which is missing in ERG8. By mutating this putative NLS in the GFP-expression constructs, we could verify the functionality of this localization signal using live cell microscopy. Moreover, alignment of ERG8 with the other isoforms also indicated that the DNA-binding domain is absent in ERG8. This DNA binding domain was recently verified by X-ray structure analysis [24] and is located close to the identified NLS of ERG1-4. This is in line with our DNA-binding studies, which revealed that the isoforms 1 to 4 bound specifically to an ERG consensus-binding site, while ERG8 did not show any significant binding.

Based on the specific localization of ERG8 in the cytosol we applied further sequence analyses searching for potential nuclear export sequences (NES). These localization signals are usually characterized by a stretch of four hydrophobic residues, typically leucines or isoleucines, separated by short spacers of 1 to 4 amino acids [40]. This structure is more

difficult to recognize as compared to NLS. Nevertheless, we could identify a putative NES in a region that is common to all ERG isoforms. In addition, we identified a potential NES in the unique C-terminus of ERG8. The presence of nuclear import as well as export signals in the ERG isoforms could be substantiated by live cell microscopy using a technique named fluorescence loss in photobleaching (FLIP), which monitors the dynamic exchange of fluorescently tagged molecules between two compartments. Repetitive bleaching of a cytosol-restricted region resulted in a decrease of nuclear fluorescence for all isoforms, demonstrating constitutive nucleo-cytoplasmic shuttling. This was even true for ERG8, which does not contain a classical NLS, but which exhibits also some weak nuclear localization. Given the fact that GFP-conjugated ERG8 is most likely above the threshold for unspecific diffusion through the nuclear pore complex, which is in the range of 30–40 kDA, we suppose the presence of a rather weak, non-classical nuclear import mechanism for ERG8. In addition to the dynamic exchange of ERG molecules between nucleus and cytosol, we also tested their mobility within a given compartment. Since most of the ERG isoforms localized primarily to the nucleus, we investigated their diffusion kinetics within this compartment using the FRAP (fluorescence recovery after photobleaching) technique. All the transcriptionally active and DNA-binding isoforms showed a similar mobility in this assay reaching a plateau at about 45% of the initial fluorescence, which implies that about 55% of the molecules are immobile within the time frame of the experiments for instance due to binding to DNA. The mobile fraction showed similar diffusion kinetics as assessed by the half time of fluorescence recovery. Again, ERG8 differed from the other ERG-isoforms. It appeared more mobile, reaching a plateau at about 62% of the initial fluorescence and showed a faster half time of fluorescence recovery. This is in line with the notion that it does not bind to DNA as suggested by our *in vitro* DNA-binding assays — and consistent with the X-ray structure analysis.

The results of the DNA binding experiments are also in line with reporter gene assays using ERG-dependent luciferase constructs. ERG 1–4 exhibited a clear transcriptional activity, while ERG8 did not lead to any significant luciferase signal similar to DNA binding mutants of an active ERG variant.

The fact that ERG8 appeared transcriptionally inactive in reporter gene assays and did not bind to ERG specific oligonucleotides implies that it is not a functional transcription factor. However, we found that it can interact physically with the other major ERG variants as assessed by FRET microscopy, which is in line with the view that ERG molecules can form homo- and heterodimers [36]. Since ERG8 did not bind to DNA, was transcriptionally inactive and localized to the cytosol, we suspected that it might act as an inhibitor of the other ERG isoforms. Indeed, we found a significant increase of endogenous ERG activity in luciferase assays after knockdown of ERG8. Interestingly, suppression of ERG8 levels by siRNA resulted in a concomitant increase in the level of active ERG in primary endothelial cells suggesting a negative feedback mechanism between expression of ERG8 and the transcriptionally active isoforms. However, even after normalization to the amount of active ERG, an inhibitory effect of ERG8 on overall ERG-dependent transcriptional activity could be observed.

This inhibitory activity of ERG8 might be caused by different mechanisms: Given that ERG8 shows physical interaction with the other isoforms, it might drag these out of the nucleus towards its own predominant localization in the cytosol. However, analysis of the localization after co-transfection of ERG8 with other isoforms indicates that only part of the molecules are interacting with each other at steady state — and that this does not change the predominant localization of the molecules. Therefore, we assume that other, or at least additional mechanisms account for an inhibitory effect of ERG8. One possibility is that ERG8 might inhibit binding of active ERG isoforms to DNA. Testing this hypothesis by analyzing the DNA-binding activity of ERG1b with increasing amounts of ERG8 revealed a rather moderate but clear reduction of ERG1b-binding to DNA (Fig. 9). However, the magnitude of this effect was rather low and was not observed for a second isoform that we tested (ERG3). Therefore, we propose that further mechanisms such as a reduced transcriptional activity of ERG dimers containing ERG8 account for its inhibitory activity. Indeed, ERG8 contains only one consensus transactivation domain, while the other isoforms contain two (Fig. 2), supporting the notion that ERG8-containing dimers would have a lower activity in recruiting the transcriptional machinery. Furthermore, ERG8 might have additional functions in the cytosol. It has been shown previously, that ERG molecules can interact with Jun. and Fos [41], both of which can localize to the cytosol at significant levels. Thus, ERG8 might also interact with these transcription factors and have specific biological roles beyond those of other ERG isoforms.

An important conclusion of our study is that ERG is actually not a single well-defined transcription factor, but rather a family of proteins arising from alternative splicing, different start codons and polyadenylation sites resulting in a diversity of protein variants. One of the isoforms that we tested, ERG8, turned out to be an inactive member of this family and to exert inhibitory functions on the other isoforms. Its biological role can be explained at least in part by the lack of a classical nuclear localization sequence, a missing DNA-binding domain and the presence of an additional nuclear export sequence in its unique C-terminus as illustrated in Fig. 11.

Since different or even contrary biological functions of ERG, such as pro-inflammatory roles in prostate cancer cells [17] as opposed to anti-inflammatory functions in endothelial cells [12,13] might be caused by differential expression of ERG isoforms, we established quantitative PCR analysis to distinguish the major variants in different cell types. This analysis revealed distinct profiles of isoform expression, which by themselves where not yet conclusive. However, calculating a ratio of transcriptionally active ERG-isoforms and ERG8 revealed an interesting general difference between non-cancer cells and four different cancer cell lines tested. In general, endothelial cells showed a higher degree of active ERGs to ERG8 as compared to the cancer cell lines. Furthermore, we observed a significant reduction of the active ERG to ERG8 ratio in the endothelial hybridoma cell line EA.hy926. This cell line was generated by fusion of HUVECs with the lung cancer cell line A549 and retains most of the characteristics of an endothelial cell line. Based on our findings, it is thus tempting to speculate that a higher expression of ERG8 in cancer cells could inhibit other ERG isoforms, which might result in a general imbalance of the transcriptional activity of the ERG isoforms expressed. This imbalance could for example, contribute to a proliferative and less apoptotic phenotype of the cancer cells. Our results also imply that a preponderance

of active ERGs might rather drive differentiation than transformation of cells. However, further studies are needed to extend this observation - and to study whether the individual active ERG-isoforms exhibit distinct biological roles for instance by driving diverse sets of target genes. Furthermore, we cannot exclude the possibility that other potentially expressed ERG isoforms, which are maybe even amplified by the same PCR-primers that we used in this study, are contributing to the observed differences in expression patterns and are exerting differential effects. Distinct functions of ERG transcription factors in different cell types might not only be caused by a differential expression of ERG-isoforms, but also by differences in the genomic accessibility for these transcription factors. We assume that this contributes strongly to the observed differences in biological roles of ERGs in various cell types. An analysis of microarray data on ERG-induced genes in endothelial cells as compared to prostate cancer cells revealed a very small overlap of just about 3% of the ERG-regulated genes (see Supplementary Information). We speculate that this striking difference in the set of target genes cannot be explained simply by different ratios of active ERGs versus ERG8 or differential expression of the individual active isoforms, but at least in addition by distinctive responsiveness of the cell types to ERGs.

Nevertheless, it would be intriguing to investigate a potential differential expression of ERG8 in a variety of cell types or diseases using microarray analyses, e.g. by re-analyzing publicly accessible databases. However, the fact that ERG8 differs from the other isoforms only in a rather short C-terminal region, hinders microarray analyses due to the lack of ERG8-specific probe sets on common microarray platforms. Therefore, we suspect that quantification of ERG8 by means of exome sequencing or proteomics might be valuable in the future to clarify whether it is correlated with cell types or disease states. In addition, microarray or RNA-sequencing analyses after specific knockdown of ERG8 in endothelial and cancer cells might address the biological function of ERG8 in more detail.

Supplementary Material

Refer to Web version on PubMed Central for supplementary material.

Acknowledgments

We thank David Bernhard, Christine Brostjan and Renate Hofer-Warbinek for generous supply of HUVEC and LEC.

Funding

This work was supported by the Austrian Science Fund (projects P23690, P27424 and SFB-F54); the City of Vienna (Hochschuljubiläumsstiftung der Stadt Wien, project H-2713/2011) and the Pakistan Overseas Scholarship Program of the Higher Education Commission, HEC, Pakistan providing scholarships for N.M., K.S. and M.I.

Abbreviations

ERG	ETS related gene
NLS	nuclear localization signal
NES	nuclear export signal

FRAP fluorescence recovery after photobleaching

FRET fluorescence resonance energy transfer

References

[1]. Murakami K, Mavrothalassitis G, Bhat NK, Fisher RJ, Papas TS. Human ERG-2 protein is a phosphorylated DNA-binding protein — a distinct member of the ETS family. Oncogene. 1993; 8:1559–1566. [PubMed: 8502479]

[2]. Rao VN, Papas TS, Reddy ES. ERG, a human ETS-related gene on chromosome 21: alternative splicing, polyadenylation, and translation. Science. 1987; 237:635–639. (New York, N.Y.). [PubMed: 3299708]

[3]. Owczarek CM, Portbury KJ, Hardy MP, O'Leary DA, Kudoh J, Shibuya K, Shimizu N, Kola I, Hertzog PJ. Detailed mapping of the ERG–ETS2 interval of human chromosome 21 and comparison with the region of conserved synteny on mouse chromosome 16. Gene. 2004; 324:65–77. [PubMed: 14693372]

[4]. Zammarchi F, Boutsalis G, Cartegni L. 5′ UTR control of native ERG and of Tmprss2: ERG variants activity in prostate cancer. PLoS One. 2013; 8:e49721. [PubMed: 23472063]

[5]. McLaughlin F, Ludbrook VJ, Cox J, von Carlowitz I, Brown S, Randi AM. Combined genomic and antisense analysis reveals that the transcription factor ERG is implicated in endothelial cell differentiation. Blood. 2001; 98:3332–3339. [PubMed: 11719371]

[6]. Randi AM, Sperone A, Dryden NH, Birdsey GM. Regulation of angiogenesis by ETS transcription factors. Biochem. Soc. Trans. 2009; 37:1248–1253. [PubMed: 19909256]

[7]. Hollenhorst PC, Ferris MW, Hull MA, Chae H, Kim S, Graves BJ. Oncogenic ETS proteins mimic activated RAS/MAPK signaling in prostate cells. Genes Dev. 2011; 25:2147–2157. [PubMed: 22012618]

[8]. Birdsey GM, Dryden NH, Amsellem V, Gebhardt F, Sahnan K, Haskard DO, Dejana E, Mason JC, Randi AM. Transcription factor ERG regulates angiogenesis and endothelial apoptosis through VE-cadherin. Blood. 2008; 111:3498–3506. [PubMed: 18195090]

[9]. Pimanda JE, Chan WY, Donaldson IJ, Bowen M, Green AR, Gottgens B. Endoglin expression in the endothelium is regulated by Fli-1, Erg, and Elf-1 acting on the promoter and a-8-kb enhancer. Blood. 2006; 107:4737–4745. [PubMed: 16484587]

[10]. Liu J, Yuan L, Molema G, Regan E, Janes L, Beeler D, Spokes KC, Okada Y, Minami T, Oettgen P, Aird WC. Vascular bed-specific regulation of the von Willebrand factor promoter in the heart and skeletal muscle. Blood. 2011; 117:342–351. [PubMed: 20980682]

[11]. Yuan L, Le Bras A, Sacharidou A, Itagaki K, Zhan Y, Kondo M, Carman CV, Davis GE, Aird WC, Oettgen P. ETS-related gene (ERG) controls endothelial cell permeability via transcriptional regulation of the claudin 5 (CLDN5) gene. J. Biolumin. Chemilumin. 2012; 287:6582–6591.

[12]. Sperone A, Dryden NH, Birdsey GM, Madden L, Johns M, Evans PC, Mason JC, Haskard DO, Boyle JJ, Paleolog EM, Randi AM. The transcription factor ERG inhibits vascular inflammation by repressing NF-kappaB activation and proinflammatory gene expression in endothelial cells. Arterioscler. Thromb. Vasc. Biol. 2011; 31:142–150. [PubMed: 20966395]

[13]. Yuan L, Nikolova-Krstevski V, Zhan Y, Kondo M, Bhasin M, Varghese L, Yano K, Carman CV, Aird WC, Oettgen P. Antiinflammatory effects of the ETS factor ERG in endothelial cells are mediated through transcriptional repression of the interleukin-8 gene. Circ. Res. 2009; 104:1049–1057. [PubMed: 19359602]

[14]. Tomlins SA, Rhodes DR, Perner S, Dhanasekaran SM, Mehra R, Sun XW, Varambally S, Cao X, Tchinda J, Kuefer R, Lee C, Montie JE, Shah RB, Pienta KJ, Rubin MA, Chinnaiyan AM. Recurrent fusion of TMPRSS2 and ETS transcription factor genes in prostate cancer. Science. 2005; 310:644–648. (New York, N.Y.). [PubMed: 16254181]

[15]. Tsuzuki S, Taguchi O, Seto M. Promotion and maintenance of leukemia by ERG. Blood. 2011; 117:3858–3868. [PubMed: 21321361]

[16]. Kaneko Y, Kobayashi H, Handa M, Satake N, Maseki N. EWS-ERG fusion transcript produced by chromosomal insertion in a Ewing sarcoma. Genes Chromosom. Cancer. 1997; 18:228–231. [PubMed: 9071576]

[17]. Wang J, Cai Y, Shao LJ, Siddiqui J, Palanisamy N, Li R, Ren C, Ayala G, Ittmann M. Activation of NF-{kappa}B by TMPRSS2/ERG fusion isoforms through Toll-like receptor-4. Cancer Res. 2011; 71:1325–1333. [PubMed: 21169414]

[18]. Li R, Pei H, Watson DK. Regulation of ETS function by protein–protein interactions. Oncogene. 2000; 19:6514–6523. [PubMed: 11175367]

[19]. Verger A, Buisine E, Carrere S, Wintjens R, Flourens A, Coll J, Stehelin D, Duterque-Coquillaud M. Identification of amino acid residues in the ETS transcription factor Erg that mediate Erg-Jun/Fos-DNA ternary complex formation. J. Biolumin. Chemilumin. 2001; 276:17181–17189.

[20]. Jaffe EA, Nachman RL, Becker CG, Minick CR. Culture of human endothelial cells derived from umbilical veins. Identification by morphologic and immunologic criteria. J. Clin. Invest. 1973; 52:2745–2756. [PubMed: 4355998]

[21]. Thomas M, Lu JJ, Ge Q, Zhang C, Chen J, Klibanov AM. Full deacylation of polyethylenimine dramatically boosts its gene delivery efficiency and specificity to mouse lung. Proc. Natl. Acad. Sci. U. S. A. 2005; 102:5679–5684. [PubMed: 15824322]

[22]. Zhang J, Thomas TZ, Kasper S, Matusik RJ. A small composite probasin promoter confers high levels of prostate-specific gene expression through regulation by androgens and glucocorticoids in vitro and in vivo. Endocrinology. 2000; 141:4698–4710. [PubMed: 11108285]

[23]. Schmid JA, Birbach A, Hofer-Warbinek R, Pengg M, Burner U, Furtmuller PG, Binder BR, de Martin R. Dynamics of NF kappa B and Ikappa Balpha studied with green fluorescent protein (GFP) fusion proteins. Investigation of GFP-p 65 binding to DNa by fluorescence resonance energy transfer. J. Biolumin. Chemilumin. 2000; 275:17035–17042.

[24]. Regan MC, Horanyi PS, Pryor EE Jr. Sarver JL, Cafiso DS, Bushweller JH. Structural and dynamic studies of the transcription factor ERG reveal DNA binding is allosterically autoinhibited. Proc. Natl. Acad. Sci. U. S. A. 2013; 110:13374–13379. [PubMed: 23898196]

[25]. Birbach A, Bailey ST, Ghosh S, Schmid JA. Cytosolic, nuclear and nucleolar localization signals determine subcellular distribution and activity of the NF-kappaB inducing kinase NIK. J. Cell Sci. 2004; 117:3615–3624. [PubMed: 15252129]

[26]. Schmid JA, Sitte HH. Fluorescence resonance energy transfer in the study of cancer pathways. Curr. Opin. Oncol. 2003; 15:55–64. [PubMed: 12490762]

[27]. Reits EA, Neefjes JJ. From fixed to FRAP: measuring protein mobility and activity in living cells. Nat. Cell Biol. 2001; 3:E145–E147. [PubMed: 11389456]

[28]. Ishikawa-Ankerhold HC, Ankerhold R, Drummen GP. Advanced fluorescence microscopy techniques — FRAP, FLIP, FLAP, FRET and FLIM. Molecules. 2012; 17:4047–4132. [PubMed: 22469598]

[29]. Sahin E, Haubenwallner S, Kuttke M, Kollmann I, Halfmann A, Dohnal AM, Chen L, Cheng P, Hoesel B, Einwallner E, Brunner J, Kral JB, Schrottmaier WC, Thell K, Saferding V, Bluml S, Schabbauer G. Macrophage PTEN regulates expression and secretion of arginase I modulating innate and adaptive immune responses. J. Immunol. 2014; 193:1717–1727. [PubMed: 25015834]

[30]. Novac N, Baus D, Dostert A, Heinzel T. Competition between glucocorticoid receptor and NFkappaB for control of the human FasL promoter. FASEB J. 2006; 20:1074–1081. [PubMed: 16770006]

[31]. Ruijter JM, Ramakers C, Hoogaars WM, Karlen Y, Bakker O, van den Hoff MJ, Moorman AF. Amplification efficiency: linking baseline and bias in the analysis of quantitative PCR data. Nucleic Acids Res. 2009; 37:e45. [PubMed: 19237396]

[32]. Pfaffl MW. A new mathematical model for relative quantification in real-time RT-PCR. Nucleic Acids Res. 2001; 29:e45. [PubMed: 11328886]

[33]. Lamber EP, Vanhille L, Textor LC, Kachalova GS, Sieweke MH, Wilmanns M. Regulation of the transcription factor Ets-1 by DNA-mediated homo-dimerization. EMBO J. 2008; 27:2006–2017. [PubMed: 18566588]

[34]. Birbach A, Gold P, Binder BR, Hofer E, de Martin R, Schmid JA. Signaling molecules of the NF-kappa B pathway shuttle constitutively between cytoplasm and nucleus. J. Biol. Chem. 2002; 277:10842–10851. [PubMed: 11801607]

[35]. Kutay U, Guttinger S. Leucine-rich nuclear-export signals: born to be weak. Trends Cell Biol. 2005; 15:121–124. [PubMed: 15752974]

[36]. Carrere S, Verger A, Flourens A, Stehelin D, Duterque-Coquillaud M. ERG proteins, transcription factors of the Ets family, form homo, heterodimers and ternary complexes via two distinct domains. Oncogene. 1998; 16:3261–3268. [PubMed: 9681824]

[37]. Jin E, Liu J, Suehiro J, Yuan L, Okada Y, Nikolova-Krstevski V, Yano K, Janes L, Beeler D, Spokes KC, Li D, Regan E, Shih SC, Oettgen P, Minami T, Aird WC. Differential roles for ETS, CREB, and EGR binding sites in mediating VEGF receptor 1 expression in vivo. Blood. 2009; 114:5557–5566. [PubMed: 19822898]

[38]. Birdsey GM, Dryden NH, Shah AV, Hannah R, Hall MD, Haskard DO, Parsons M, Mason JC, Zvelebil M, Gottgens B, Ridley AJ, Randi AM. The transcription factor Erg regulates expression of histone deacetylase 6 and multiple pathways involved in endothelial cell migration and angiogenesis. Blood. 2012; 119:894–903. [PubMed: 22117042]

[39]. Furusato B, Tan SH, Young D, Dobi A, Sun C, Mohamed AA, Thangapazham R, Chen Y, McMaster G, Sreenath T, Petrovics G, McLeod DG, Srivastava S, Sesterhenn IA. ERG oncoprotein expression in prostate cancer: clonal progression of ERG-positive tumor cells and potential for ERG-based stratification. Prostate Cancer Prostatic Dis. 2010; 13:228–237. [PubMed: 20585344]

[40]. la Cour T, Gupta R, Rapacki K, Skriver K, Poulsen FM, Brunak S. NESbase version 1.0: a database of nuclear export signals. Nucleic Acids Res. 2003; 31:393–396. [PubMed: 12520031]

[41]. Basuyaux JP, Ferreira E, Stehelin D, Buttice G. The Ets transcription factors interact with each other and with the c-Fos/c-Jun complex via distinct protein domains in a DNA-dependent and -independent manner. J. Biolumin. Chemilumin. 1997; 272:26188–26195.

[42]. Reddy ES, Rao VN, Papas TS. The erg gene: a human gene related to the ets oncogene. Proc. Natl. Acad. Sci. U. S. A. 1987; 84:6131–6135. [PubMed: 3476934]

[43]. Youvan DC, Coleman WJ, Silva CM, Petersen J, Bylina EJ, Yang MM. Calibration of fluorescence resonance energy transfer in microscopy using genetically engineered GFP derivatives on nickel chelating beads. Biotechnology et alia. 1997; 3:1–18.

[44]. Feige JN, Sage D, Wahli W, Desvergne B, Gelman L. PixFRET, an ImageJ plug-in for FRET calculation that can accommodate variations in spectral bleed-throughs. Microsc. Res. Tech. 2005; 68:51–58. [PubMed: 16208719]

Europe PMC Funders Author Manuscripts

Europe PMC Funders Author Manuscripts

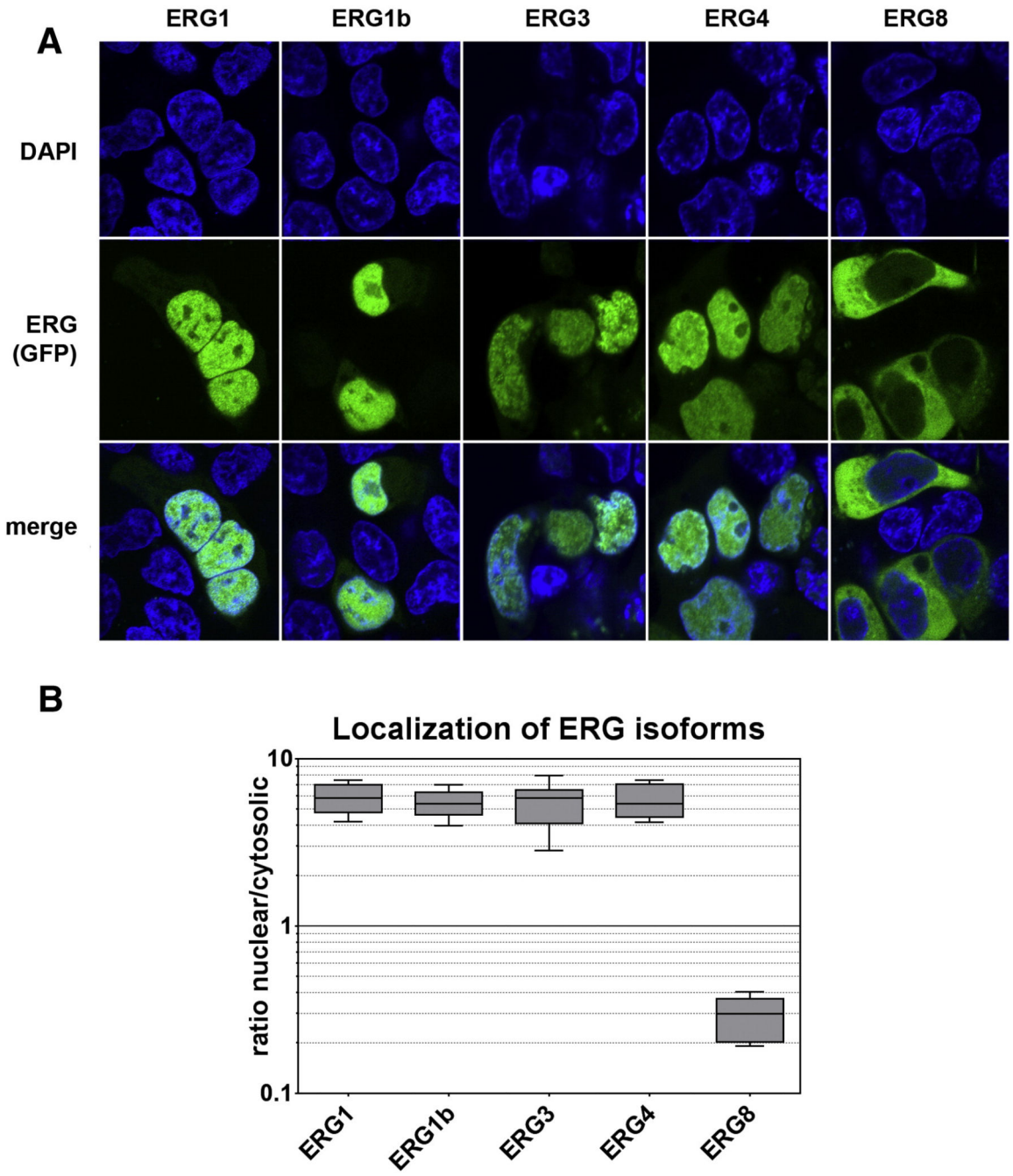

Fig. 1.

Subcellular localization of ERG isoforms. (A) GFP tagged versions of ERG isoforms (EGFP–ERG1, –ERG1b, –ERG3, –ERG4, –ERG8) were transfected in HEK293 cells and nuclei were stained with DAPI. Images of live cells were taken with a Nikon A1 R + confocal microscope. (B) Box-Whiskers Plot of the nuclear to cytosolic fluorescence ratio showing the 10–90 percentiles on a logarithmic scale ($n \geq 17$).

Europe PMC Funders Author Manuscripts

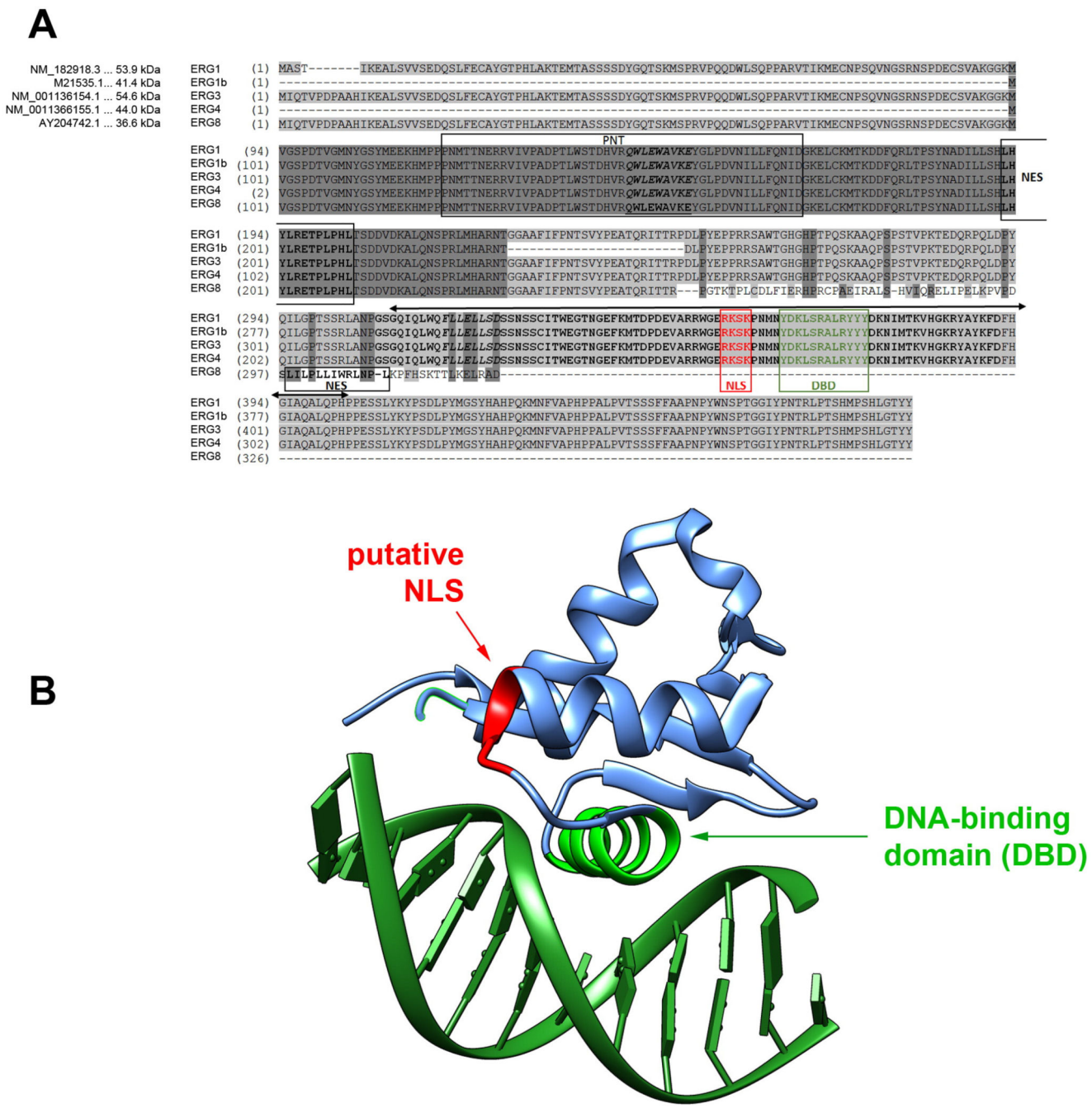

Fig. 2.

Sequence comparison of the ERG isoforms used in this study. (A) Sequence alignment of ERG isoforms by VectorNTI-software: bold: ETS domain; bold and italics: postulated transactivation domains; boxed and labeled with “PNT”: PNT domain; red, boxed and labeled with “NLS”: putative nuclear localization sequence (NLS); boxed and labeled with “NES”: putative nuclear export sequences (NES); green, boxed and labeled with “DBD”: DNA binding domain. Double-headed arrows indicate the fragment that was used for X-ray structure analysis shown in B. ERG1, ERG3, ERG4 and ERG8 are described in [3], ERG1b

is the original ERG1 representing the first reported ERG family member [42]. NCBI reference numbers and molecular weights of the proteins are indicated on the upper left side. (B) DNA bound structure of ERG (4IRI) showing the putative NLS in red and the DNA-binding helix in green (visualized with Chimera 1.8 software).

Europe PMC Funders Author Manuscripts

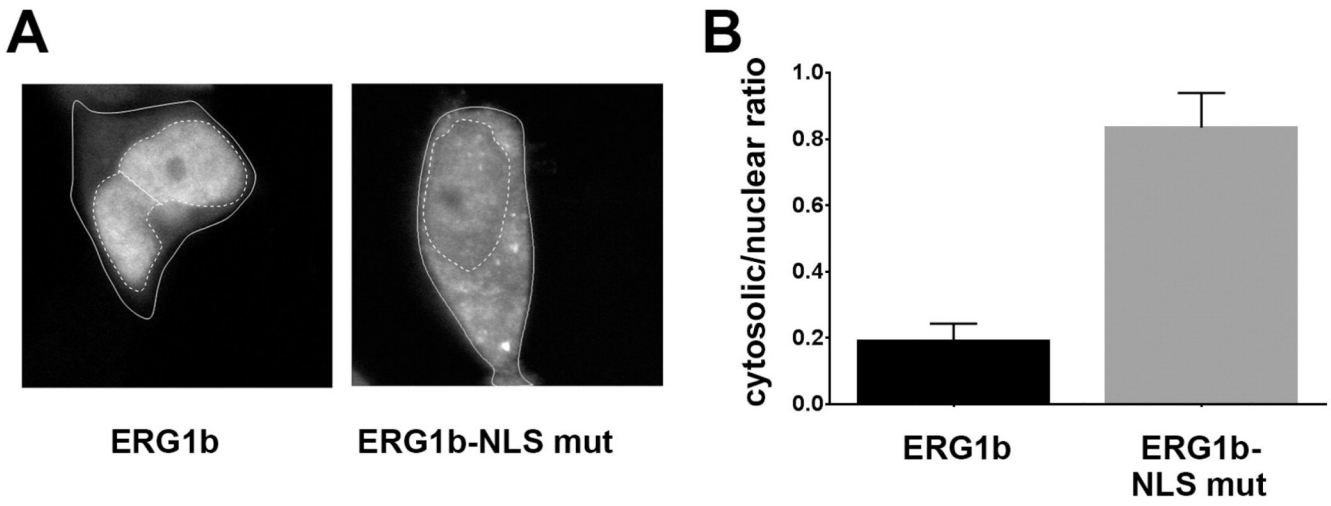

Fig. 3.

Verification of the putative nuclear localization sequence. (A) GFP-tagged-ERG1b and its NLS mutant (ERG1b-NLS mut.) were transfected into cells and assessed by microscopy. Cell borders are outlined with a continuous line; nuclei are indicated by a dashed line. (B) Quantification of cytosolic to nuclear fluorescence intensity ratios for ERG1b and the ERG1b-NLS mutant as indicated. (n = 12, $p < 0.0001$, error bars represent SEM).

Europe PMC Funders Author Manuscripts

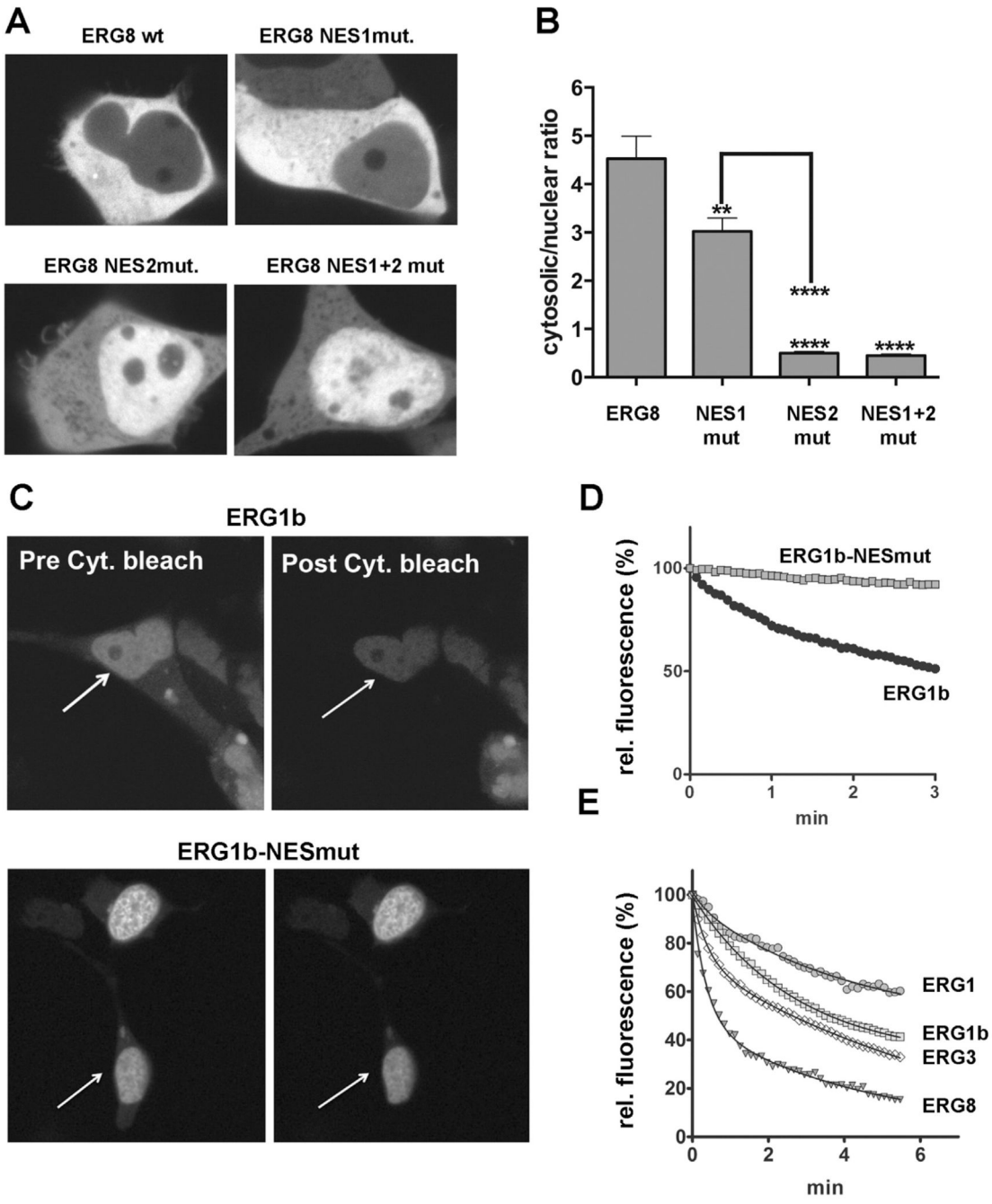

Fig. 4.

Nuclear export sequences in ERG isoforms and nucleo-cytoplasmic shuttling. (A) EGFP–ERG8 and mutants of the two putative NES (NES1mut., NES2mut.), as well as double mutants (NES1 + 2mut.), were transfected into HEK293 cells and analyzed by fluorescence microscopy. (B) Quantification of cytosolic to nuclear fluorescence ratios of cells transfected as in (A). n = 11, $p < 0.0001$. (C) Fluorescence loss in photobleaching (FLIP) analysis of EGFP-ERG1b and its nuclear export sequence mutant (EGFP-ERG1b-NESmut). HEK293 cells were seeded on coverslips and transfected with GFP tagged versions of

ERG1b or ERG1b with a mutated NES. A region of interest in the cytoplasm was bleached with high laser power and fluorescence intensities were recorded as described in the Materials and methods section. A decrease of fluorescence in the non-bleached compartment (the nucleus) indicates shuttling between nucleus and cytoplasm (fluorescence loss in photobleaching, FLIP). Nuclei of cells, in which the cytosol has been bleached, are indicated by arrows. Images before cytosol bleaching (Pre Cyt. bleach) and after cytosol bleaching (Post Cyt. bleach) are shown. (D) Quantification of the nuclear fluorescence intensity in the course of repetitive cytosolic bleaching for ERG1b and the ERG1b-NES mutant. One representative experiment out of six is shown. (E) FLIP analysis of the nucleo-cytosolic shuttling of the ERG isoforms 1, 1b, 3, and 8. A representative experiment is shown (n = 4).

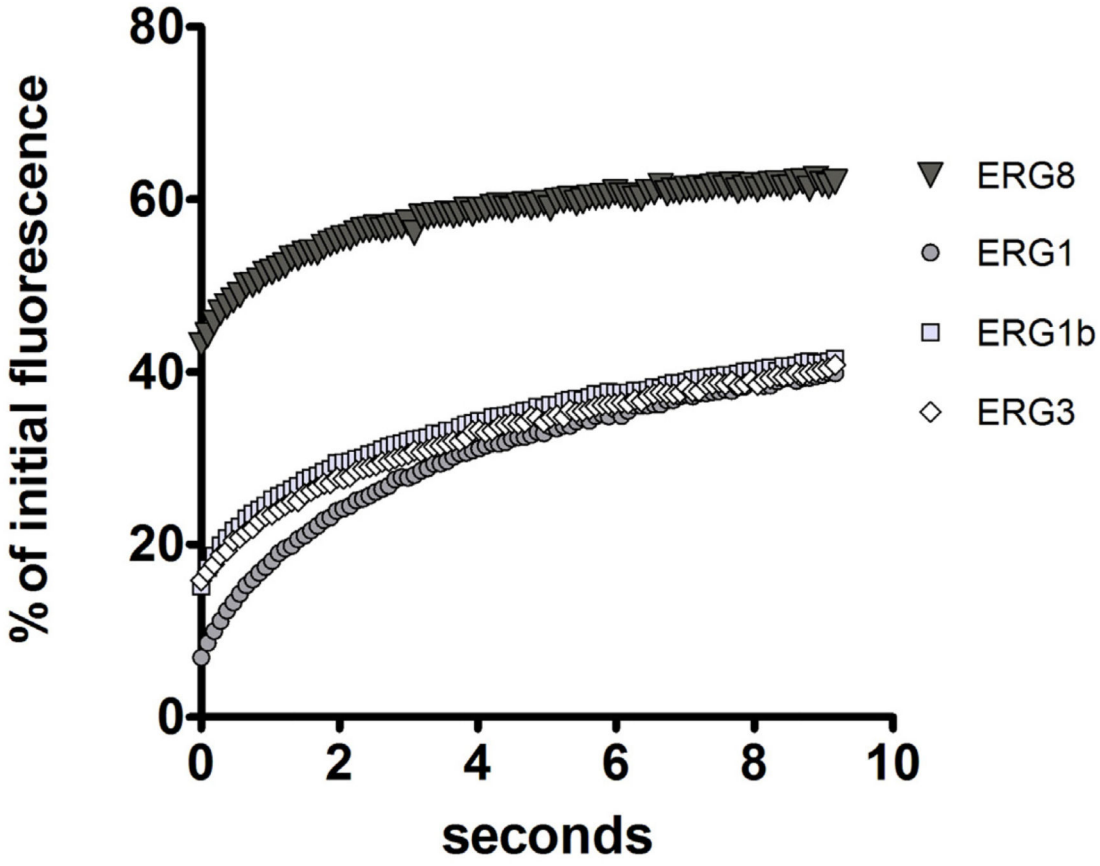

Best-fit values	ERG1	ERG1b	ERG3	ERG8
Plateau	41.39	42.56	42.39	61.65
Half-time	2.389	2.512	2.825	1.498
95% Confidence Intervals				
Plateau	40.92 to 41.86	41.99 to 43.13	41.85 to 42.93	61.44 to 61.87
Half-time	2.291 to 2.495	2.358 to 2.689	2.675 to 2.992	1.420 to 1.586
Goodness of Fit				
R^2	0.9961	0.9915	0.9948	0.9887

Fig. 5.

Mobility of ERG isoforms in the nucleus. Evaluation of the fluorescence recovery after photobleaching (FRAP) to determine the mobility in the nucleus. As for FLIP, HEK293 cells were seeded on coverslips and transfected with GFP tagged versions of ERG isoforms as indicated. Live cells were examined with a laser-scanning microscope. A region of interest in the nucleus was bleached with high laser power and fluorescence recovery in the same region was recorded. The mean of four experiments is shown. Non-linear regression analysis using a one-phase association algorithm (least square fit) was performed with the software GraphPad Prism 5.0 ™. The table below the graph shows the results of the analysis.

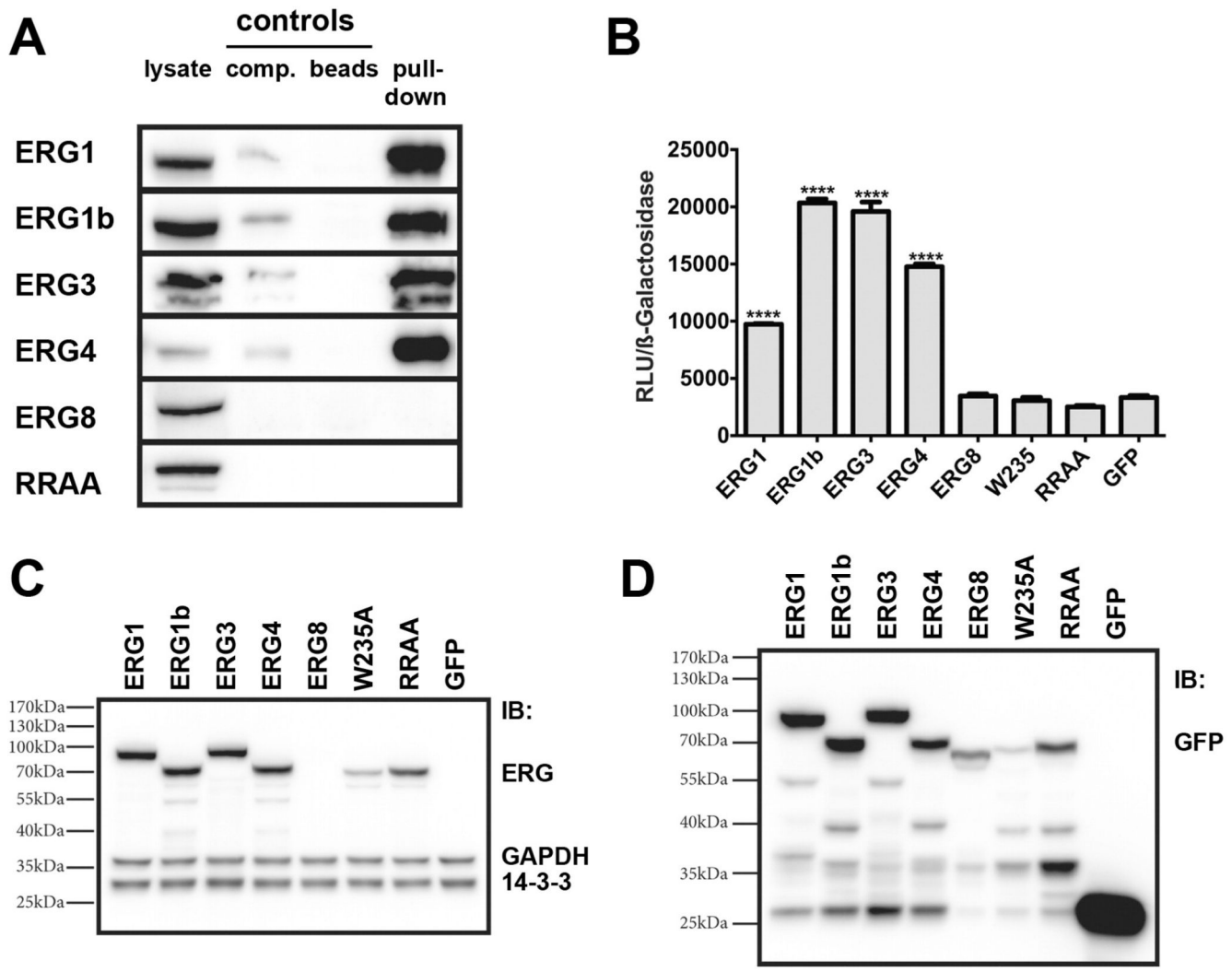

Fig. 6.

DNA-binding and transcriptional activities of ERG isoforms. (A) DNA binding as assessed by ABCD assays (Avidin Biotin Complex with DNA). HEK293 cells were transfected with various isoforms as indicated (ERG1, ERG1b, ERG3, ERG4, ERG8, RRAA-mutant) and the lysates subjected to ABCD assays using oligonucleotides with ERG-binding sites as described in the Materials and methods section. Cell lysates were used as positive control for expression of the ERG-isoform (lysate); a 10-fold molar excess of a non-biotinylated oligonucleotide served as competitor control (comp.) and cell lysates incubated with streptavidin-beads in the absence of any oligonucleotide as negative control (beads). The pull-down samples show binding of ERG isoforms to a biotinylated oligonucleotide containing known ERG binding sites (pull-down). (B) Reporter gene assay to determine the transcriptional activities of ERG-isoforms. HEK293 cells were transfected with a luciferase reporter containing three ERG-binding sites (3× ERG-Luc) in combination with a constitutively expressing β-galactosidase construct for normalization either in the absence of any ERG-isoform (GFP, control) or in presence of ERG-isoforms as indicated. In addition, known non-functional ERG variants with mutations in the DNA-binding domain were tested

(W235R- and RRAA-mutants as indicated and described in the Materials and methods section). Error bars represent standard deviation (n = 3). (C, D) Western blots using an ERG (C) or a GFP antibody (D) in samples used for luciferase assays.

Europe PMC Funders Author Manuscripts

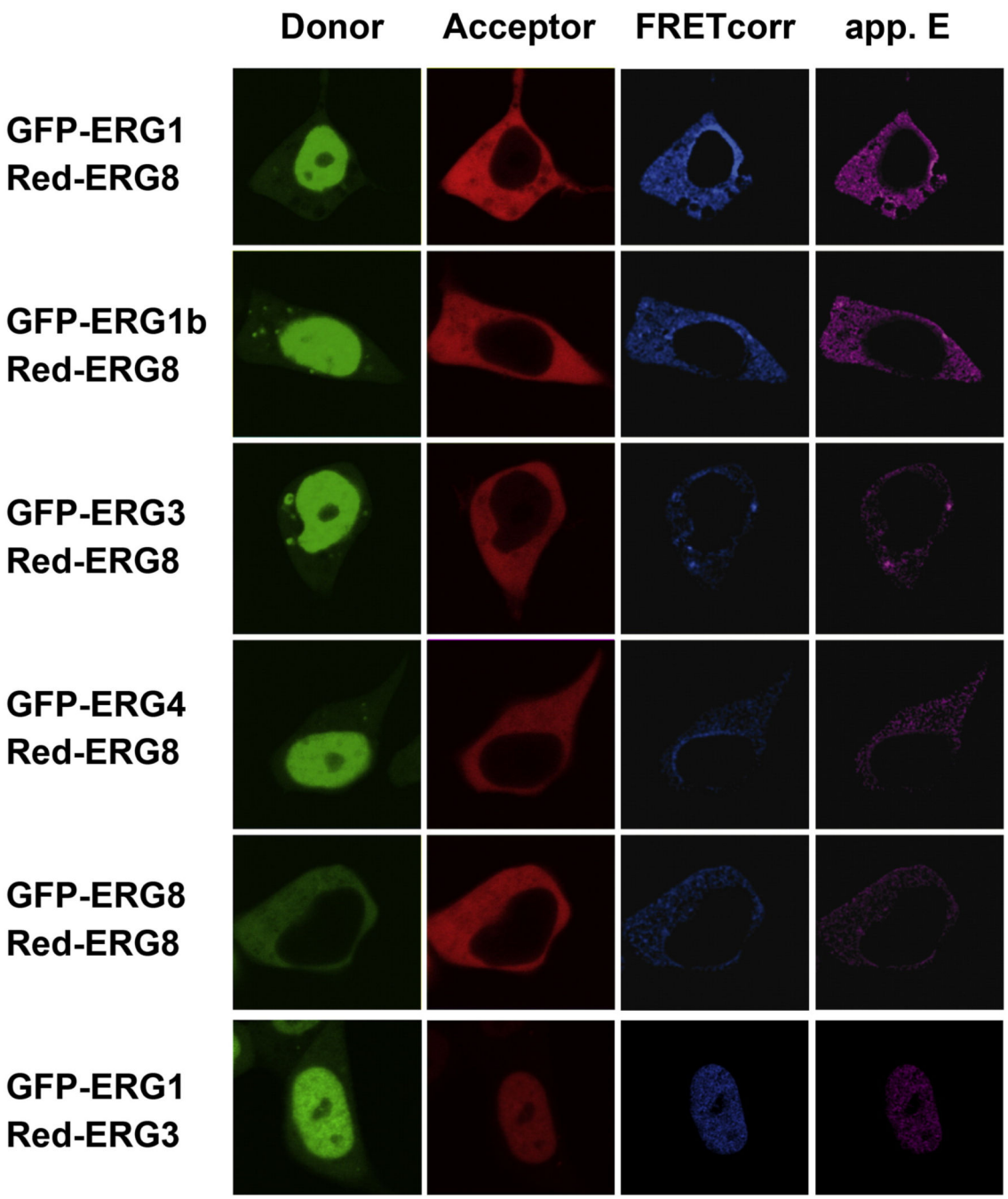

Fig. 7.

ERG8 interacts with other ERG isoforms. Representative FRET microscopy analysis of ERG isoforms 1 to 4 binding to ERG8. Cells were transfected with ERG-isoforms tagged with GFP or mDsRed (red) as indicated and subjected to 3-Filter FRET microscopy as described in the Materials and methods section. A corrected FRET image according to [43] was calculated (FRETcorr), as well as an image showing the apparent FRET efficiency (app. E) as described in [44]. An example of the interaction between two active isoforms is shown

at the last row (ERG1/ERG3). The last two columns (FRET corr and app. E) are shown in a pseudocolor mode to visualize low values.

Europe PMC Funders Author Manuscripts

Europe PMC Funders Author Manuscripts

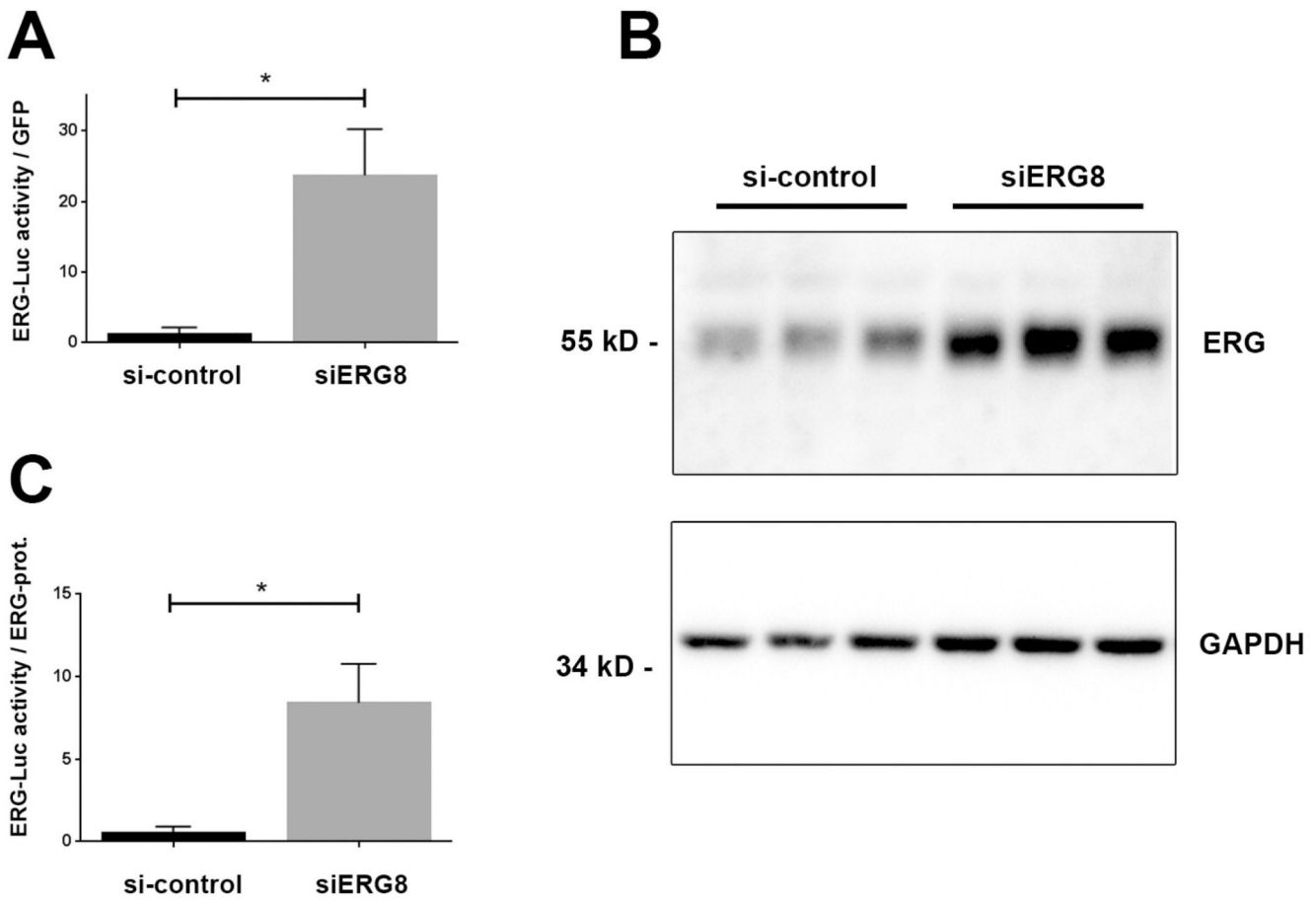

Fig. 8.

Effect of ERG8 knockdown on the transcriptional activity of endogenous ERG isoforms in endothelial cells. HUVECs were transfected with scrambled control si-RNA (si-control) or siRNA targeting the unique C-terminus of ERG8 (siERG8) in combination with an improved ERG-dependent luciferase reporter construct (ERG-Nanoluc) and a constitutively expressing GFP-reporter for normalization. (A) ERG-luciferase activity in cell extracts normalized to GFP fluorescence. (B) Western blot analysis of the extracts shown in (A) with an anti-ERG antibody (upper panel), recognizing endogenous ERG1-4 but not ERG8, which lacks the epitope, as well as with GAPDH antibodies (lower panel) as loading control. (C) ERG luciferase activity of the extracts, when normalized to the ERG-protein band shown in (B). n = 3, error bars represent SEM; an asterisk indicates statistical significance with an unpaired students t-test.

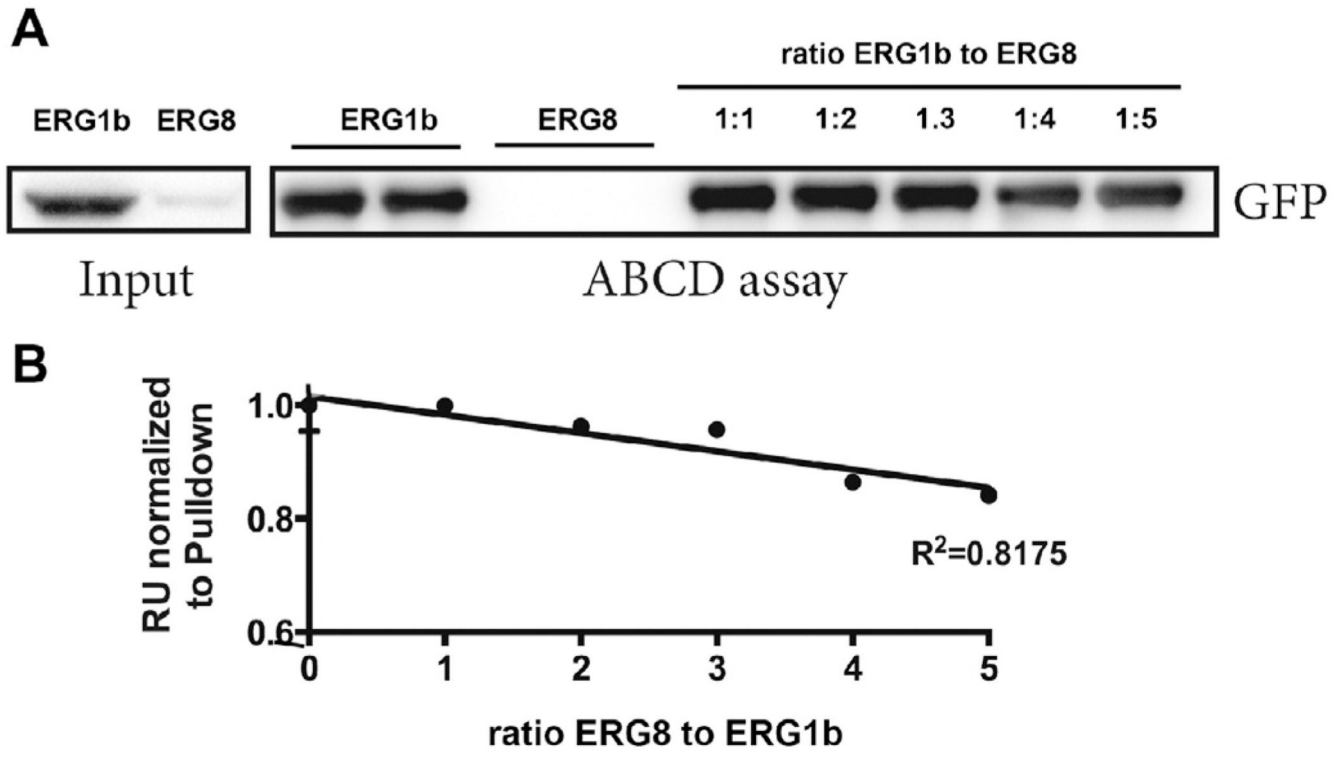

Fig. 9.

Effect of ERG8 on the DNA binding activity of ERG1b. (A) Lysates of cells transfected with either ERG1b or ERG8 were mixed at different ratios (1:0, 0:1, 1:1, 1:2, 1:3, 1:4, 1:5) and subjected to an ABCD DNA-binding assay with biotinylated oligonucleotides containing ERG-binding sites. After pull-down with streptavidin-beads, bound ERG molecules were detected by SDS-PAGE and Western blots. (B) Quantification of Western blots as shown in (A). ERG1b DNA-binding capability decreased with increasing amounts of ERG8.

Europe PMC Funders Author Manuscripts

Europe PMC Funders Author Manuscripts

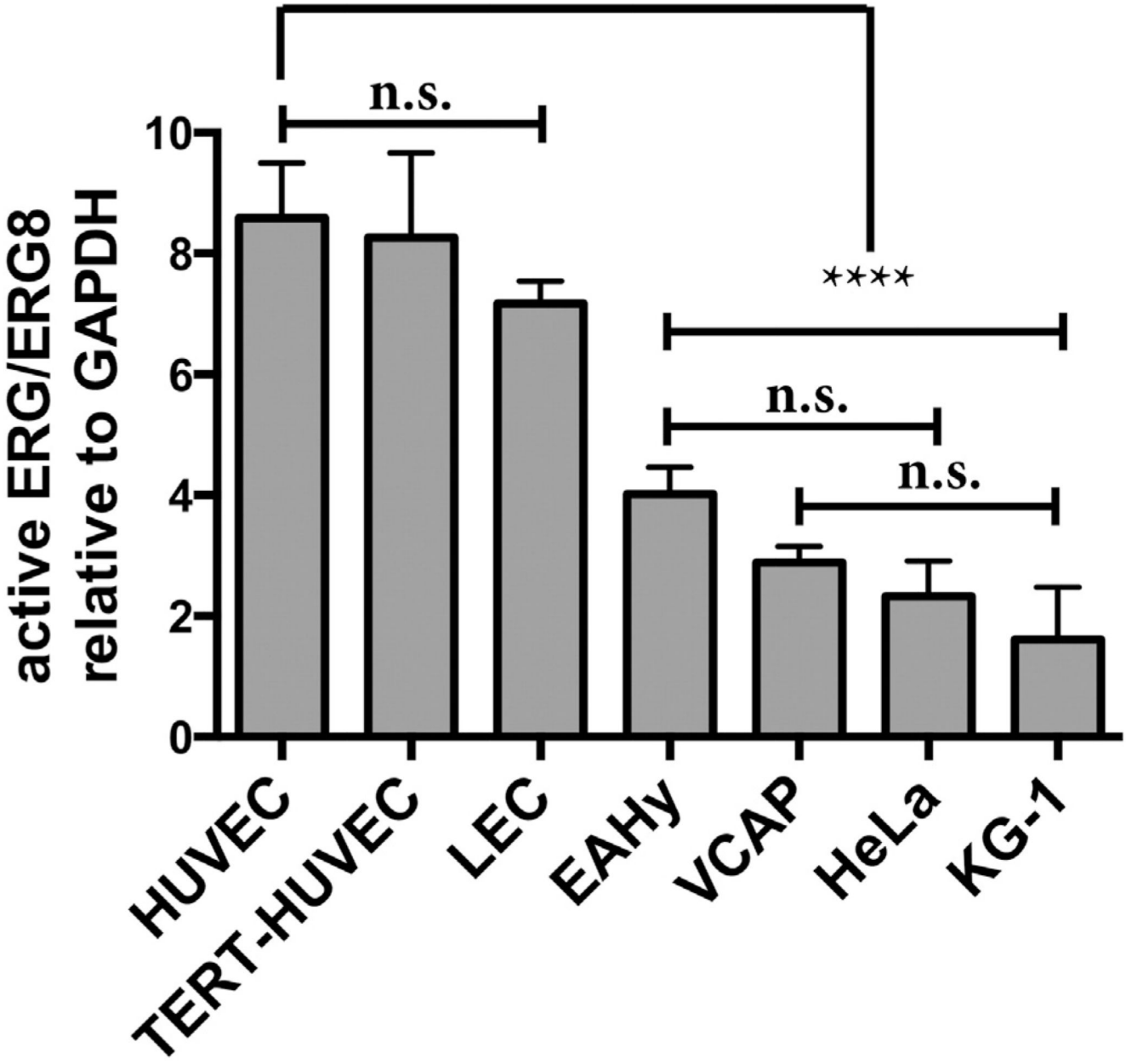

Fig. 10.

Ratio of total active ERG-isoform mRNA to ERG8-mRNA. mRNA was extracted from the different cell types indicated, reverse transcribed and subjected to quantitative PCR as described in the Materials and methods section (n = 3, error bars represent standard deviations). One-way ANOVA and Dunnett's multiple comparison tests were performed with GraphPad Prism software. Significance of difference is indicated (n.s.: non-significance applies to comparison between HUVECS with TERT-HUVECS and LEC cells; $p < 0.0001$ applies to comparisons between HUVECs with EaHy, VCAP, HeLa, and KG-1 cells).

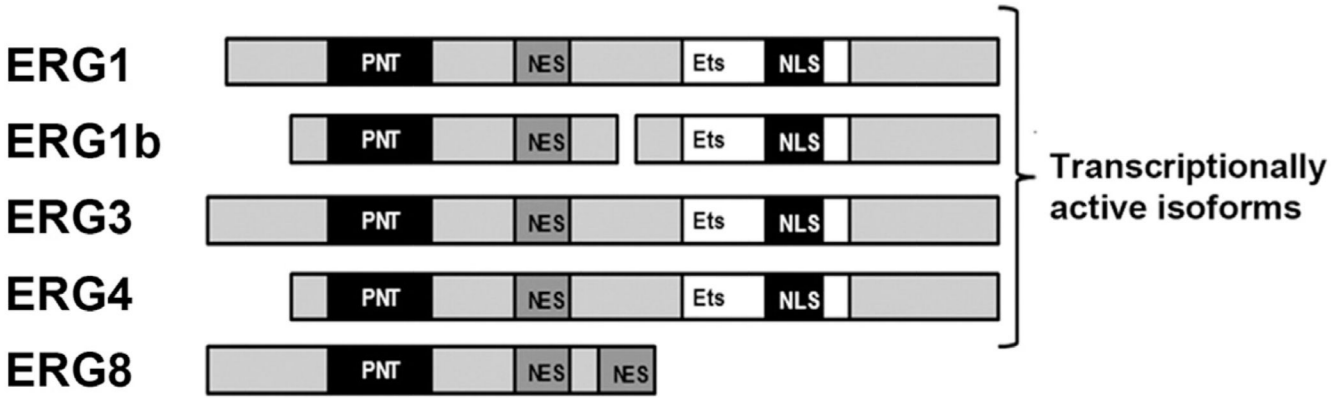

Fig. 11.

Summary of ERG isoforms illustrating the identified NES and NLS domains in combination with the known PNT and ETS domains.